Available online at www.sciencedirect.com

jmr&t Journal of Materials Research and Technology

journal homepage: www.elsevier.com/locate/jmrt

Thermally conductive and electrically resistive acrylonitrile butadiene styrene (ABS)/boron nitride composites: Optimal design using a multi-criteria decision-making approach

László Lendvai [a,b,*], Tej Singh [c], Daniele Rigotti [b], Alessandro Pegoretti [b]

[a] Department of Materials Science and Engineering, Széchenyi István University, H-9026, Győr, Hungary
[b] Department of Industrial Engineering, University of Trento, 38123 Trento, Italy
[c] Savaria Institute of Technology, Eötvös Loránd University, H-9700, Szombathely, Hungary

ARTICLE INFO

Article history:
Received 18 July 2023
Accepted 17 September 2023
Available online 20 September 2023

Keywords:
Acrylonitrile butadiene styrene
Boron nitride
Thermal conductivity
Electrical resistivity
Mechanical properties
Optimization

ABSTRACT

The purpose of this work is to propose a decision-making algorithm to select the optimal composite material for thermally conductive but electrically insulating applications, such as microelectronic packaging heat sinks, diodes, and other electronic devices. In particular, an algorithm based on the criteria importance through inter-criteria correlation (CRITIC) and additive ratio assessment (ARAS) methods are used to evaluate several conflicting attributes. The evaluated samples were acrylonitrile butadiene styrene (ABS) composites filled with 0–30 vol% of boron nitride (BN) particles and prepared through melt compounding. The performance attributes considered through testing were heat conductivity, electrical resistivity, density, hardness, and tensile properties (Young's modulus, tensile strength, and elongation). As expected, the composite containing 30 vol% BN exhibited the highest heat conductivity, electrical resistivity, and Young's modulus. Meanwhile, unfilled ABS had the highest elongation at break, tensile strength, and lowest density. With respect to hardness, the 1 vol% BN-loaded composite proved to be superior. Therefore, the experimental data revealed a considerable compositional dependence with no obvious trend. The optimal composition was identified by adopting the CRITIC-ARAS multi-criteria decision-making algorithm, based on which the 30 vol% BN-containing composite was dominant among all the prepared samples. A validation through other decision-making techniques was performed to support the robustness of the proposed technique. Additionally, a sensitivity analysis was carried out on several weight exchange scenarios to see the stability of the ranking results.

* Corresponding author. Department of Materials Science and Engineering, Széchenyi István University, H-9026, Győr, Hungary.
E-mail address: lendvai.laszlo@sze.hu (L. Lendvai).

https://doi.org/10.1016/j.jmrt.2023.09.165

1. Introduction

Recent years have seen an immense development in communication technology and electronic technology. Due to the current trend of integration and miniaturization of various electronic devices, heat dissipation has become a major challenge in the field of electronic packaging, diodes, energy storage, and aerospace [1,2]. As a consequence of the intensive heat accumulation in such products, the proper dissipation of any excess heat is critical in order to maintain good performance, service lifetime, and stable operation. Various 5G network devices, tablet computers, light-emitting diodes (LEDs), batteries, and many other devices of everyday life are involved in this problem [3–5]. Besides the sufficient thermal management capabilities, there are several parallel requirements against the materials used in the above-mentioned fields, such as excellent electrical insulation, low density, decent mechanical properties, and good processability [5,6]. Polymeric materials have been widely used for such purposes; however, their relatively low intrinsic thermal conductivity (0.1–0.4 W/mK) makes them ever less appropriate, which greatly hinders their application in today's electronic devices of higher energy density [6]. Currently, the most common technique to achieve thermally conductive polymer-based materials is to pair plastics with different appropriate fillers, thereby fabricating thermally conductive polymer composites. Potential additives for such composites can be various metallic, carbonaceous, and ceramic fillers [2,7]. In this respect, the development of all-organic polymer composites is an interesting approach, since carbon-based additives, such as graphene nanoplatelets can effectively improve the thermal conductivity without compromising the mechanical and physical properties of the polymer matrix [8,9]. Carbon-based, and metallic additives, however, only provide an optimal solution when the electrical insulation is not a requirement; for electrically insulating purposes ceramic particles are the optimal choice. Among the ceramics, a number of candidates have been studied in the past, including aluminum oxide (Al_2O_3) [10,11], boron nitride (BN) [2,12–14], aluminum nitride (AlN) [15–17] and silicon carbide (SiC) [18]. The resulting properties of such multicomponent materials are determined by various factors, such as the type of filler, its shape, concentration, distribution, and the applied manufacturing process. Among the various ceramic fillers, boron nitride is the most promising additive owing to its excellent electrical insulating and thermal conductivity properties [15].

Kovacs and Suplicz [19] fabricated thermally conductive composites with a polypropylene (PP) matrix and used talc and BN particles as fillers to achieve the desired properties. For compression molded samples, the conductivity of 30 vol% BN-filled PP increased to 1.14 W/mK compared to the initial 0.25 W/mK value of neat PP. Talc-filled samples exhibited a considerably lower improvement, peaking at 0.6 W/mK at the same filler loading. The authors have also shown that the same composites prepared by injection molding possess much lower conductivity compared to the compression molded ones, due to the formation of a shell-core structure within the specimens. Cheewawuttipong et al. [20] prepared PP-based composites with 15 vol%, 21 vol%, and 29 vol% BN content using two different BN types; small (1–2 μm) and large (7–10 μm). The study reported an improving heat conductivity at increased BN content with the larger particles being superior to the smaller ones in this respect. The authors attributed this to the formation of a conductive network, which was more easily formed when using larger particles. A maximum conductivity of 2 W/mK was achieved for the samples reinforced with 30 vol% large BN powder. Zhou et al. [21] studied the thermal, electrical, and mechanical properties of boron nitride–filled composites using epoxy as a matrix. The authors applied a surface treatment on BN with γ–glycidoxypropyltrimethoxysilane and subsequently mixed it with epoxy. The thermal conductivity of the polymer increased from 0.22 W/mK to 1.2 W/mK when filled with 50 wt% pristine BN and further to 1.34 W/mK when surface treatment was also applied. Meanwhile, the volume resistivity decreased from 52×10^{14} Ω cm to 6×10^{14} Ω cm. Considering the mechanical properties, it was presented that the addition of BN increases the modulus of the samples, albeit at the cost of strength and ductility. Wei et al. [22] investigated the effect of BN nanoplatelets on the mechanical and conductive properties of high-density polyethylene (HDPE)-based composites containing up to 15 wt% filler. The Young's modulus of HDPE increased from 741 MPa to 1066 MPa at maximum filler content, which was also paired with improved yield stress from 23.2 MPa to 25.2 MPa. This latter was ascribed to the outstanding exfoliation of the nanosheets. Interestingly, however, the thermal conductivity values of the composites were reduced slightly when compared to the unfilled HPDE. The authors attributed this drop to the fact that a lower number of thermally conductive pathways formed due to the high levels of exfoliation and dispersion of BNs.

Acrylonitrile-butadiene-styrene (ABS) is a widely used engineering thermoplastic copolymer. ABS owns a number of beneficial features, including high impact resistance, outstanding surface finish, moderate tensile strength, decent modulus, wear resistance, and chemical resistance [23]. Furthermore, its non-crystalline nature enables a low shrinkage during melt processing and therefore allows high dimensional stability. On the other hand, its intrinsically low thermal conductivity hinders its use in many fields, including miniaturized electronic devices with high energy density [24]. This shortcoming may be eliminated using fillers that were studied in the literature with other plastics as described above.

The reviewed literature increasingly emphasizes that the selection of components and their relative proportions generally affect the final properties of the composite material. Therefore, designing the correct formulation that provides the desired results is a common problem for engineers and decision-makers. In recent years, many scholars have explored different perspectives on the issue of formulation optimization. However, in many circumstances, decision-makers have to deal with the issue of multiple competing evaluation criteria, further complicating the process of choosing the best among viable composite material alternatives. In dealing with these complex challenges, "multi-criteria decision-making" (MCDM) is one of the reliable methods [25,26]. Several studies have investigated the

ranking of composite materials by evaluating various alternatives. A few of them include VIKOR (*vise kriterijumska optimizacija kompromisno resenje* – multi-criteria optimization compromise solution), MOORA (multi-objective optimization on the basis of ratio analysis), SAW (simple additive weighting), multiplicative exponent weighting (MEW), COPRAS (complex proportional assessment), WASPAS (weighted aggregated sum product assessment), CRITIC (criteria importance through inter-criteria correlation), and ARAS (additive ratio assessment) [27–31]. Proposed by Zavadskas et al. [32], the ARAS method has proven effective in handling intricate and uncertain decision-making scenarios. The effectiveness of the ARAS method can be achieved by assessing the utility level of each alternative and considering the outstanding values of the selected criteria. The ARAS methodology was successfully used in solar water heater design by Khargotra et al. [33], smartwatch selection by Gülçin et al. [34], engine operating parameters optimization by Balki et al. [35], catering supplier selection by Yan-Kai Fu [36], and sustainable biomass crop selection by Mishra et al. [37]. Its widespread use and rapid expansion result from its straightforward approach, both in concept and implementation. It produces reasonably accurate and acceptable ranking results among various recommended alternatives based on their performance concerning specified criteria [38]. CRITIC, an objective weighting approach proposed by Diakoulaki et al. [39], utilizes the contrast intensity of criteria to determine their respective weights. This contrast intensity is evaluated as the standard deviation. Additionally, the approach calculates the contradictions among the criteria by employing the correlation coefficient [40]. In addition, Aytekin et al. [41], Jovčić and Průša [42], Sultana and Dhar [43], and Ayyldz and Ekinci [44] reported the use of the integrated CRITIC-ARAS approach in the food business, selection of logistics providers, milling of alloys, and in the software development industry, respectively.

In the present study, hexagonal boron nitride-filled ABS-based composites were prepared and tested for their thermal conductivity, electrical resistivity, hardness, tensile mechanical properties, and density. As seen in the results, choosing the optimal composite was challenging since each composite performed differently for the investigated properties. Therefore, an integrated CRITIC-ARAS-based MCDM is proposed to select the best candidate from the existing composite alternatives with the highest satisfaction of the evaluated conflicting properties. Sensitivity analysis and a comparison of the ranking outcomes with other MCDM approaches that are currently in use have also been performed in order to assess the robustness and consistency of the proposed CRITIC-ARAS methodology.

2. Materials and methods

2.1. Materials

ABS pellets of grade Magnum 3453 with a melt flow rate of 15 g/10 min (220 °C/10 kg) were purchased from Trinseo (Wayne, Pennsylvania, USA). Hexagonal boron nitride powder Hebofill 482 with an average particle size of 30 μm and a purity of higher than 98.5% was obtained from Henze BNP (Lauben, Germany).

2.2. Preparation of the samples

The ABS/BN composites were produced by batchwise melt compounding using a counter-rotating Haake Polylab mixer (Vreden, Germany) with a mixing chamber of 50 cm^3. The melt mixing was performed at 190 °C and 60 rpm for a total of 10 min. At first, ABS was added to the mixing chamber, while BN particles were dosed after 3 min, when the measured torque was stabilized. A total of seven samples were prepared with 0, 1, 3, 5, 10, 20 and 30 vol% of BN. The designation code and the composition of the investigated materials are summarized in Table 1.

The prepared ABS/BN composites were compression molded into sheets of ~2 mm thickness using a Carver laboratory press 4122 (Wabash, IN, USA) at a temperature of 190 °C for 5 min. Specimens for characterization were cut out of the compression molded sheets with a laboratory-scale CNC mill.

2.3. Characterization and testing

The Shore D hardness (criterion C1) of the samples was measured with a Hildebrand Durometer OS-2 model (Wendlingen, Germany) hardness tester. The average values of hardness were calculated from the results of seven consecutive measurements.

Quasi-static tensile tests were performed using an Instron 5969 (Norwood, MA, USA) electro-mechanical testing machine following the ISO 527 standard. The tests were carried out at room temperature on dumbbell-shaped specimens of type 1BA. The machine was equipped with a 10 kN load sensor. The initial deformation was recorded with a clip-on extensometer of Instron (Norwood, MA, USA). The crosshead speed was set to 10 mm/min. The average values of tensile strength (criterion C2), Young's modulus (criterion C3), and elongation at break (criterion C4) values were calculated from the results of five consecutive measurements.

The morphology of the fabricated samples was examined by using a Hitachi S-3400 N (Tokyo, Japan) scanning electron microscope (SEM) equipped with a secondary electron detector. Observations were made at an accelerating voltage of 10 kV on the fracture surfaces obtained by the tensile tests. Prior to the SEM analysis, the surfaces of the specimens were coated with gold, using a sputtering technique with a Quorum

Table 1 – Designation and formula of the composites by volume and weight.

Designation	ABS (vol%)	ABS (wt.%)	BN (vol%)	BN (wt.%)
ABS	100	100	0	0
1BN	99	98.2	1	1.8
3BN	97	94.7	3	5.3
5BN	95	91.3	5	8.7
10BN	90	83.2	10	16.8
20BN	80	68.8	20	31.2
30BN	70	56.3	30	43.7

SC7620 apparatus (Laughton, UK) to avoid charging during the electron beam scanning.

The density of the samples was measured on the basis of Archimedes' principle in ethanol at 23 °C using a Gibertini E42 (Modena, Italy) precision digital balance, with a sensitivity of 10^{-4} g.

The electrical volume resistivity of the ABS/BN samples was measured by using a Keithley 8009 resistivity test chamber (Ohio, USA) coupled with a Keithley 6517A high-resistance meter (Ohio, USA).

The thermal conductivity measurements were performed using a Netzsch LFA 467 HyperFlash (Selb, Germany) laser flash thermal conductivity meter at a temperature of 25 °C under an inert N_2 atmosphere. The flash method is a widely recognized technique for the determination of thermophysical properties: thermal diffusivity, specific heat, and thermal conductivity of solid materials.

2.4. *Proposed hybrid CRITIC-ARAS approach*

Fig. 1 lays out the steps involved in the hybrid CRITIC-ARAS decision-making process. Part 1 covers the alternatives, criteria, and decision matrix; Part 2 covers the CRITIC technique for weighting criteria; Part 3 covers the ARAS method for ranking; and Part 4 covers rank validation and weight sensitivity.

2.4.1. *Part 1: alternatives, criteria, and decision matrix*

For the initialization of any MCDM, firstly the alternatives and criteria used in the ranking analysis are determined. Thereafter, a decision matrix is structured using alternatives and criteria. Consider '*m*' alternatives and '*n*' evaluation criteria a decision matrix ($D = [d_{ij}]_{m\times n}$), which can be structured as shown in Eq. (1):

$$D = [d_{ij}]_{m\times n} = \begin{bmatrix} d_{11} & d_{12} & \dots & d_{1j} & \dots & d_{1n} \\ d_{21} & d_{22} & \dots & d_{2j} & \dots & d_{2n} \\ \vdots & \vdots & \dots & \vdots & \dots & \vdots \\ d_{i1} & d_{i2} & \dots & d_{ij} & \dots & d_{in} \\ \vdots & \vdots & \dots & \vdots & \dots & \vdots \\ d_{m1} & d_{m2} & \dots & d_{mj} & \dots & d_{mn} \end{bmatrix} \quad (1)$$

where d_{ij} in the decision matrix indicates the value of *i*th alternative in the *j*th criterion.

2.4.2. *Part 2: CRITIC method for weight calculation*

The objective weighting technique CRITIC was suggested by Diakoulaki et al. [39], which can consider correlations between all specified criteria. The contrast intensities (measured in terms of criterion standard deviations) were also incorporated into this procedure and mixed with correlation analysis weights [39,40]. The CRITIC technique is as follows:

Step 1: Decision matrix normalization as follows (Eq. (2));

$$\Re_{ij} = \begin{cases} \dfrac{d_{ij} - d_j^{\min}}{d_j^{\max} - d_j^{\min}} \ \text{if } j \in n_b \\ \dfrac{d_j^{\max} - d_{ij}}{d_j^{\max} - d_j^{\min}} \ \text{if } j \in n_c \end{cases} \quad (2)$$

where n_b represent beneficial and n_c represent beneficial non-beneficial criteria.

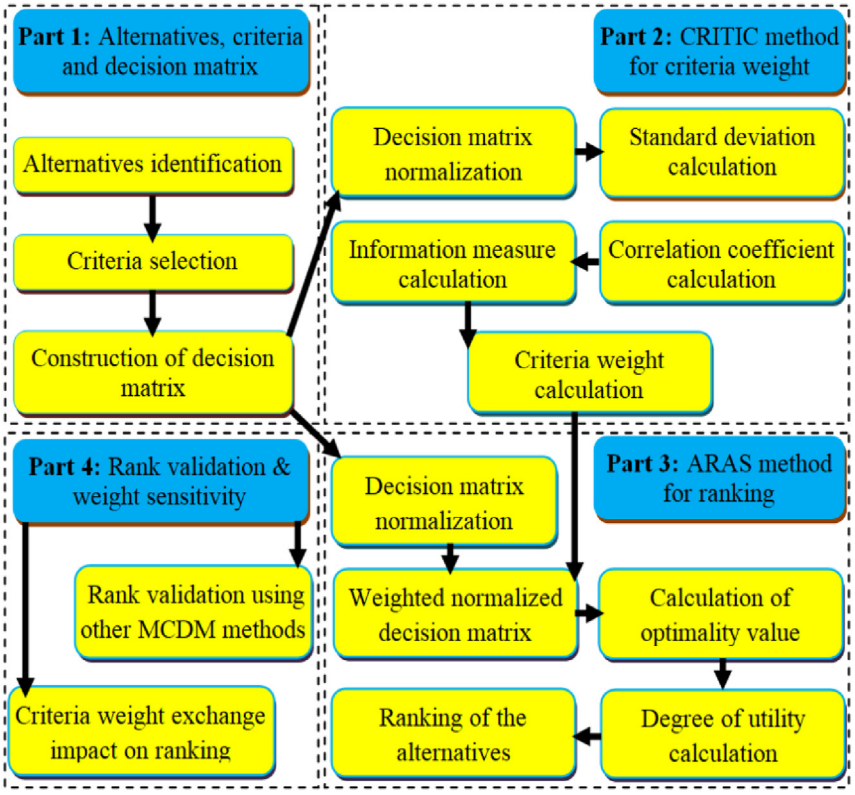

Fig. 1 – Proposed CRITIC-ARAS algorithm.

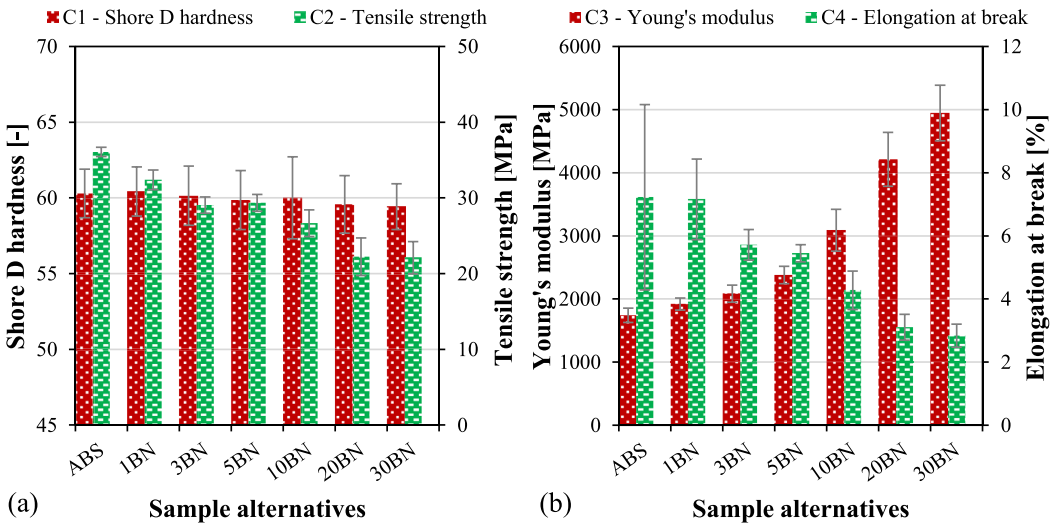

Fig. 2 – Variation of C-1: Shore D hardness; C-2 Tensile strength (a) and C-2: Young's modulus; C-4: Elongation at break (b).

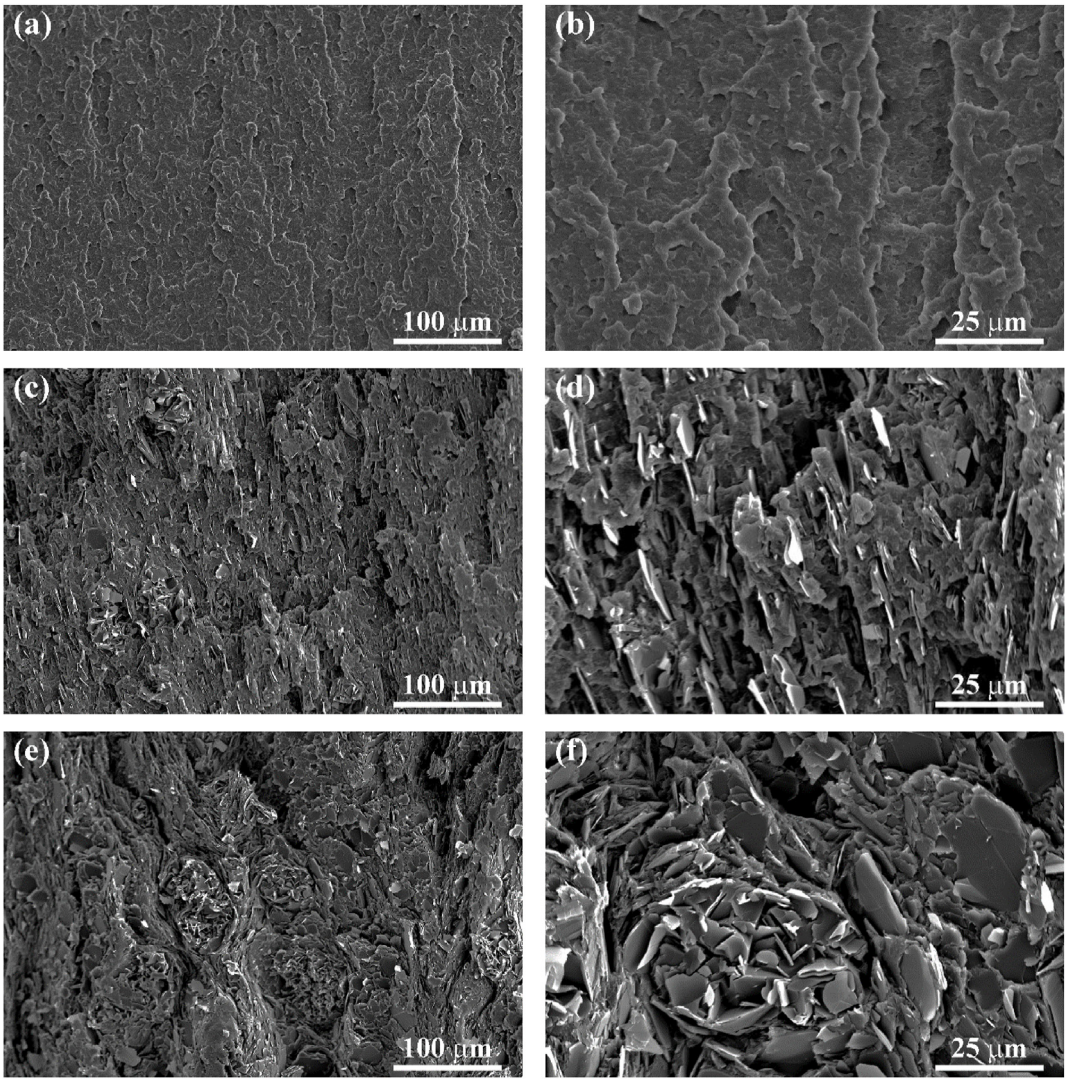

Fig. 3 – Tensile fracture surface morphology of samples ABS (a, b) 10BN (c, d) and 30BN (e, f) at lower and higher magnifications.

Step 2: Criteria standard deviation (φ_j) computed as follows (Eq. (3));

$$\varphi_j = \sqrt{\frac{1}{m-1}\sum_{i=1}^{m}\left(\Re_{ij} - \overline{d}_j\right)^2}; j = 1, \cdots, n \tag{3}$$

where $\overline{d}_j$ represents the mean of the jth criterion.

Step 3: Determining the correlation coefficient (χ_{jk}) between the two criteria say j and k as follows (Eq. (4));

$$\chi_{jk} = \frac{\sum_{i=1}^{m}\left(\Re_{ij} - \overline{d_j}\right)\left(\Re_{ik} - \overline{d_k}\right)}{\left(\sum_{i=1}^{m}\left(\Re_{ij} - \overline{d_j}\right)^2 \sum_{i=1}^{M}\left(\Re_{ik} - \overline{d_k}\right)^2\right)^{\frac{1}{2}}} j, k = 1, 2, \cdots, n \tag{4}$$

where $\overline{d_j}$ and $\overline{d_k}$ represent the mean of the jth and kth criterion, respectively.

Step 4: Criteria index value (Φ_j) computed as follows (Eq. (5));

$$\Phi_j = \varphi_j \sum_{j=1}^{n}\left(1 - \chi_{jk}\right);\ j = 1, 2, \cdots, n \tag{5}$$

Step 5: Computing the CRITIC weights (ω_j) for each criterion as shown in Eq. (6);

$$\omega_j = \frac{\varphi_j}{\sum_{j=1}^{n}\varphi_j};\ j = 1, 2, \cdots, n \tag{6}$$

2.4.3. *Part 3: ARAS method for ranking*

By measuring the degree of utility of each alternative relative to the ideal best choice, Zavadskas et al. [32] proposed ARAS, a practical and sophisticated MCDM approach, for making the best decision. The steps that make up the ARAS method's process are as follows:

Step 1: Decision matrix formation; the ARAS technique differs from other MCDM approaches because the decision matrix has a line of optimal values for each criterion. For m alternatives and n criteria, the decision matrix is structured as follows (Eq. (7));

$$D' = \left[d'_{ij}\right]_{m\times n} = \begin{bmatrix} d_{01} & d_{02} & \cdots & d_{0j} & \cdots & d_{0n} \\ d_{11} & d_{12} & \cdots & d_{1j} & \cdots & d_{1n} \\ d_{21} & d_{22} & \cdots & d_{2j} & \cdots & d_{2n} \\ \vdots & \vdots & \cdots & \vdots & \cdots & \vdots \\ d_{i1} & d_{i2} & \cdots & d_{ij} & \cdots & d_{in} \\ \vdots & \vdots & \cdots & \vdots & \cdots & \vdots \\ d_{m1} & d_{m2} & \cdots & d_{mj} & \cdots & d_{mn} \end{bmatrix} \tag{7}$$

where d_{0j} = optimal value of jth criterion. The following equations (Equation (8)) were used to obtain the jth criterion's ideal value.

$$d_{0j} = \begin{cases} \max\limits_{i} d_{ij} \text{ if } j \in n_b \\ \min\limits_{i} d_{ij} \text{ if } j \in n_c \end{cases} i = 1, 2, \cdots m; j = 1, 2, \cdots n \tag{8}$$

where n_b represent beneficial and n_c represent non-beneficial criteria.

Step 2: Decision matrix normalization as follows (Eq. (9));

$$\overline{\Re}_{ij} = \begin{cases} \dfrac{d_{ij}}{\sum_{i=0}^{m} d_{ij}} \text{ if } j \in n_b \\ \dfrac{1/d_{ij}}{\sum_{i=0}^{m} 1/d_{ij}} \text{ if } j \in n_c \end{cases} \tag{9}$$

where n_b represent beneficial and n_c represent non-beneficial criteria.

Step 3: Decision matrix weighted normalization as follows (Eq. (10));

$$Z_{ij} = \overline{\Re}_{ij} \times \omega_j \ i = 0, 1, \cdots m;\ j = 1, 2, \cdots n \tag{10}$$

where Z_{ij} represents the ith alternatives weighted normalized performance rating with respect to the jth criterion.

Step 4: Optimality function (μ_i) determination for each alternative by applying the following formula (Eq. (11)):

$$\mu_i = \sum_{j=1}^{n} Z_{ij} \ i = 0, 1, \cdots m \tag{11}$$

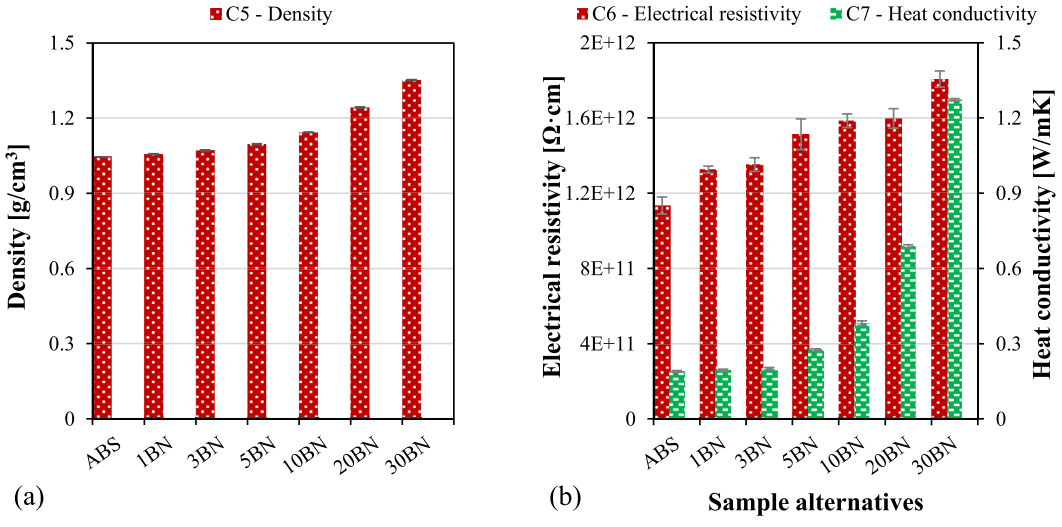

Fig. 4 – Variation of C-5: Density (a) and C-6: Electrical resistivity; C-7: Heat conductivity (b).

Step 5: Computation of utility degree (θ_i) of alternatives using the following equation (Eq. (12)).

$$\theta_i = \frac{\mu_i}{\mu_0} \; i = 0, 1, \cdots m \tag{12}$$

where μ_0 = optimality function for the optimal criterion obtained from Equation (11). Obviously, the calculated θ_i values vary from 0 to 1 (1 for μ_0).

Step 6: Alternatives ranking.

The recommended options are listed in ascending order by θ_i, thereafter Equation (13) is used to get the best alternative (A^*):

$$A^* = \left\{ A_i | \max_i \; \theta_i \right\} i = 0, 1, \cdots m \tag{13}$$

2.4.4. *Part 4: rank validation and weight sensitivity*

The suggested CRITIC-ARAS technique was verified by contrasting its results with other well-known MCDM strategies (including SAW, WASPAS, VIKOR, COPRAS, MOORA, and MEW). As part of the sensitivity study, the criteria weights found by the CRITIC method were switched, and a new ranking analysis was done for each change using the ARAS method. The rank correlation was also used to compare the alternatives' rankings from different methods and weight-exchange situations with the suggested methodology's rankings. This was done by calculating the Spearman correlation coefficient (CC) using Eq. (14) [26].

$$CC = 1 - \frac{6\sum_{i=1}^{m} \Delta_i^2}{m(m^2 - 1)} \tag{14}$$

where, Δ_i = rank difference and m = alternatives.

3. Results and discussion

3.1. *Influence of boron nitride on the evaluated properties*

Figs. 2–4 show the results of the prepared samples in accordance with the chosen criteria. The Shore D hardness (C1) of the prepared composites is illustrated in Fig. 2a. It exhibits a rather small reduction as a function of boron nitride content; however, the hardness values of all samples were within the deviation range at ~60 Shore D. Similar results of slightly reducing hardness in the presence of ceramic particles were already reported by other studies previously for various polymer composites [45–48]. In the literature, this kind of behavior is attributed to the fact that at high BN concentrations, a larger and denser filler network of soft BN agglomerates is formed inside the polymer matrix. In such a system, the basically weak filler-filler interactions become increasingly more dominant relative to the filler-polymer interactions, ultimately leading to a decrease in hardness and other mechanical properties. The tensile strength (C2) of the ABS samples also decreased, when BN was introduced, as shown in Fig. 2a. The neat polymer exhibited a strength of 36 MPa, which gradually dropped with increasing filler content, bottoming at 22 MPa for sample 30BN. It is suggested that there is a limited interfacial adhesion between the components, which does not enable an effective stress transfer from the ABS chain molecules to the BN particles [49]. This is also supported by the reduced elongation at break (C4) values recorded for the boron nitride-filled composites compared to the neat ABS matrix (Fig. 2b). Hence, according to

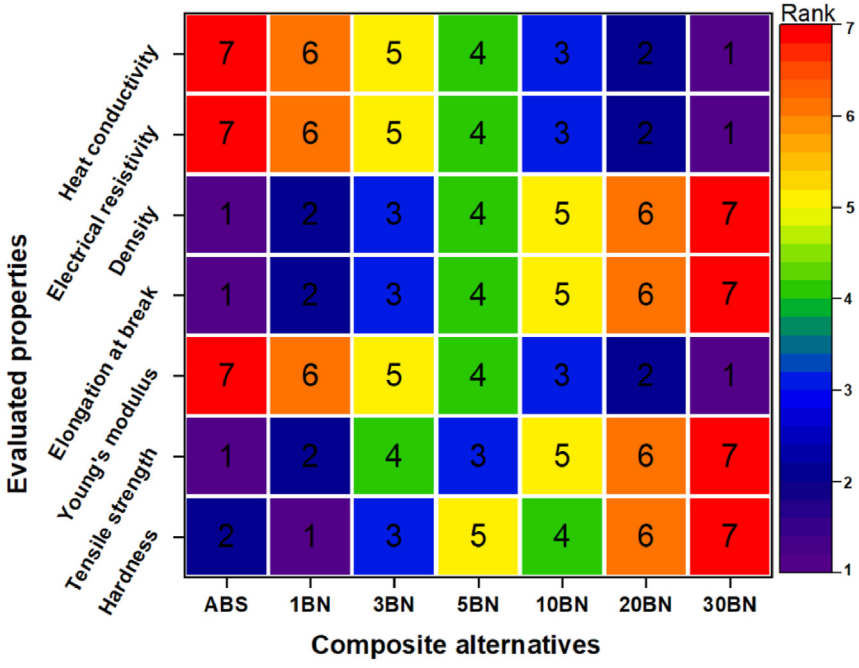

Fig. 5 – Ranking of composite alternatives based on individual criteria.

Table 2 – Decision matrix for CRITIC analysis.

Alternatives	C1	C2	C3	C4	C5	C6	C7
ABS	60.29	36.08	1739.29	7.22	1.047	1.13×10^{12}	0.189
1BN	60.43	32.39	1919.45	7.16	1.056	1.33×10^{12}	0.194
3BN	60.14	29.05	2083.80	5.72	1.071	1.35×10^{12}	0.200
5BN	59.86	29.35	2379.20	5.45	1.096	1.51×10^{12}	0.275
10BN	60.00	26.65	3089.31	4.27	1.143	1.59×10^{12}	0.382
20BN	59.57	22.23	4213.42	3.11	1.243	1.60×10^{12}	0.688
30BN	59.43	22.11	4946.84	2.83	1.352	1.81×10^{12}	1.273

the literature, the resulting composites exhibit a less ductile behavior, and the ceramic filler does not concur with strength enhancement [7].

The Young's modulus (C3) of the fabricated samples can be seen in Fig. 2b. Neat ABS exhibited a modulus of 1740 MPa, which increased remarkably when it was paired with BN powder. Even 1 vol% of BN particles enabled a relative improvement of over 10%, while the incorporation of 30 vol% BN resulted in Young's modulus value of 4947 MPa, which is almost threefold compared to ABS. This gradual increase in stiffness can be attributed to the rigid characteristics of the ceramic filler, which hinders the motion of the chain molecules when mechanical load is applied. The reason for the modulus of the BN-filled samples showing an opposite trend compared to tensile strength and hardness is the fact that – unlike the latter properties – modulus is not much influenced by the interfacial adhesion of the components since it is measured at relatively low deformation, where there is insufficient dilation to cause interface separation. Therefore, the individual properties of the components are much more vital in this regard [50].

SEM analysis was performed to further evaluate the tensile performance of the BN-filled ABS samples and presented in Fig. 3. Fig. 3a and b shows the fractured surface of pure ABS, which appeared to be smooth with no pores or voids being present. Also, no signs of plastic deformation can be detected on the surface, which is in good agreement with the relatively low elongation at break values measured for all samples. Fig. 3c and d shows the fractured surface of sample 10BN. Apparently, at 10 vol% BN loading the dispersion of the filler particles is rather good, even though some small agglomerates can be detected. In the case of individual nanoplatelets embedded into the ABS matrix, their orientation seems uniform; they are parallel to the planes of the compression molded sheets, and as such, barely any contact between them can be observed. On the other hand, the bundles of BN particles, the so-called agglomerates appear to be randomly oriented. For the 30BN composite (Fig. 3e and f) the same conclusions can be drawn, however, the ratio of BN particles present in the form of agglomerates is much higher in this case, which also means more randomness in the orientation of the particles. Besides, agglomerates generally act as failure sites in polymeric nanocomposites, which explains the major drop in tensile strength and also supports the claims made considering the reduction in hardness.

According to Fig. 4a, the density (C5) of the samples gradually increased with growing BN content, which is something that was expected considering that the density of BN (1.88 g/cm^3) greatly exceeds that of ABS (1.04 g/cm^3). Accordingly, the lowest density was exhibited by the unfilled polymer, while the sample 30BN showed the highest one (1.35 g/cm^3).

Boron Nitride (BN) is a two-dimensional particle with excellent chemical, thermal, mechanical, and optical properties, which make it especially attractive for electronics applications. BN has a large electrical bandgap between 5.2 and 5.9 eV [51,52] and a small dielectric constant that ranges between 2 and 4 [53], which are highly advantageous over metallic fillers and carbon nanomaterials when the electrical resistivity and dielectric constant of the composite are concerned.

Electrical resistivity (C6) plays a crucial role in nanocomposites intended for use as thermal interface materials in electronic devices [54]. In this study, the electrical conductivity of the ABS/BN nanocomposites was investigated by measuring their volume resistivity, and the corresponding results are illustrated in Fig. 4b. It was observed that the

Table 3 – Results of the CRITIC method.

Alternatives	Normalized decision matrix						
	C1	C2	C3	C4	C5	C6	C7
ABS	0.8600	1.0000	0.0000	1.0000	1.0000	0.0000	0.0000
1BN	1.0000	0.7359	0.0562	0.9863	0.9705	0.2941	0.0046
3BN	0.7100	0.4968	0.1074	0.6583	0.9213	0.3235	0.0101
5BN	0.4300	0.5183	0.1995	0.5968	0.8393	0.5588	0.0793
10BN	0.5700	0.3250	0.4209	0.3280	0.6852	0.6765	0.1780
20BN	0.1400	0.0086	0.7713	0.0638	0.3574	0.6912	0.4603
30BN	0.0000	0.0000	1.0000	0.0000	0.0000	1.0000	1.0000
Standard deviation (φ_j), index value (Φ_j), and weight (ω_j)							
φ_j	0.3667	0.3659	0.3860	0.4058	0.3735	0.3277	0.3700
Φ_j	2.1682	2.1576	3.0651	2.3848	2.2924	2.5810	2.8485
ω_j	0.1239	0.1233	0.1752	0.1363	0.1310	0.1475	0.1628

Table 4 – Decision matrix for ARAS analysis.

Alternatives	C1	C2	C3	C4	C5	C6	C7
A0	60.43	36.08	4946.84	7.22	1.047	1.81×10^{12}	1.273
ABS	60.29	36.08	1739.29	7.22	1.047	1.13×10^{12}	0.189
1BN	60.43	32.39	1919.45	7.16	1.056	1.33×10^{12}	0.194
3BN	60.14	29.05	2083.80	5.72	1.071	1.35×10^{12}	0.200
5BN	59.86	29.35	2379.20	5.45	1.096	1.51×10^{12}	0.275
10BN	60.00	26.65	3089.31	4.27	1.143	1.59×10^{12}	0.382
20BN	59.57	22.23	4213.42	3.11	1.243	1.60×10^{12}	0.688
30BN	59.43	22.11	4946.84	2.83	1.352	1.81×10^{12}	1.273

volume resistivity of the ABS/BN nanocomposites was higher than that of the pristine ABS, especially with the incorporation of BN as a filler (1.13×10^{12} Ω cm). Specifically, when the ABS/BN nanocomposite contained a loading of 30 vol% BN filler, the volume resistivity increased to 1.81×10^{12} Ω cm, resulting in a notable 60% relative increment compared to the neat ABS. These findings align with similar results reported in the scientific literature for thermoplastic systems loaded with BN [55–57].

The thermal conductivity (C7) of the ABS/BN composites was measured using the laser flash method, which is a commonly employed technique in scientific research. The results obtained showed that the thermal conductivity of the ABS/BN composites increased with an increase in the loading of BN, as depicted in Fig. 4b. When the BN loading reached its highest content of 30 vol%, the thermal conductivity reached 1.272 ± 0.004 W/mK, representing a significant percentage increase (~570%) compared to the neat ABS, which exhibited a thermal conductivity of 0.189 ± 0.003 W/mK. This observed trend is well-documented in the scientific literature for various polymer and boron nitride systems [58–60].

In addition, Fig. 5 displays the rankings of the samples based on their effectiveness for each evaluated property. Fig. 5 clearly shows that variations in BN loading considerably impact the assessed characteristics. None of the investigated composites has outperformed the others in terms of all analyzed properties simultaneously. For instance, pure ABS excelled in density, elongation at break, and tensile strength. Nevertheless, it performed poorly regarding electrical resistivity, heat conductivity, and Young's modulus. Composite 1BN has the second lowest electrical resistivity, thermal conductivity, and Young's modulus but the highest hardness, second-highest elongation at break, and highest tensile strength. Composite 30BN outperformed all other materials in terms of electrical resistivity, heat conductivity, and Young's modulus, but it ranked last in elongation at break, tensile strength, hardness, and density. Therefore, these sample alternatives were ranked using an integrated CRITIC-ARAS-based MCDM technique to select the best candidate that meets on the whole all of these conflicting features. The evaluated properties, including density, electrical resistivity, thermal conductivity, tensile mechanical properties, and hardness were taken as selection criteria. For thermally conductive composites, the criteria hardness (C1), tensile strength (C2), Young's modulus (C3), elongation at break (C4), electrical resistivity (C6), and heat conductivity (C7) were considered as beneficial (i.e., higher-the-better) features. At the same time, density (C5) was considered to be non-beneficial (i.e., the lower-the-better).

3.2. *Ranking of the alternatives*

3.2.1. *CRITIC results*

Following the procedure steps described in section 2.4, the criteria weights were determined using the CRITIC approach. First, using $\Re_{ij}$ values in accordance with Eq. (2), the matrix (given in Table 2) is normalized. The results are shown in Table 3. The standard deviations (φ_j) were then determined for each criterion using Eq. (3) and are displayed in Table 3 as well. The index values (Φ_j) were then determined using Eq. (5), and they are also shown in Table 3. The criteria weights are then obtained using Eq. (6) as follows: C1; Shore D hardness = 0.1239, C2; tensile strength = 0.1233, C3; tensile modulus = 0.1752, C4; elongation at break = 0.1363, C5; density = 0.1310, C6; electrical resistivity = 0.1475 and C7; heat conductivity = 0.1628 as listed in Table 3.

3.2.2. *Alternatives ranking*

The ranking of composite alternatives was evaluated using the ARAS technique after the weights of different criteria were calculated. Table 4 displays the findings of the composite

Table 5 – The normalized decision matrix.

Alternatives	C1	C2	C3	C4	C5	C6	C7
A0	0.1259	0.1542	0.1954	0.1680	0.1341	0.1492	0.2845
ABS	0.1256	0.1542	0.0687	0.1680	0.1341	0.0932	0.0422
1BN	0.1259	0.1385	0.0758	0.1666	0.1330	0.1096	0.0434
3BN	0.1253	0.1242	0.0823	0.1331	0.1311	0.1113	0.0447
5BN	0.1247	0.1255	0.0940	0.1268	0.1281	0.1245	0.0615
10BN	0.1250	0.1139	0.1220	0.0993	0.1228	0.1311	0.0854
20BN	0.1241	0.0950	0.1664	0.0724	0.1130	0.1319	0.1538
30BN	0.1238	0.0945	0.1954	0.0658	0.1038	0.1492	0.2845

Table 6 – The weighted normalized decision matrix.

Alternatives	C1	C2	C3	C4	C5	C6	C7
A0	0.0156	0.0190	0.0342	0.0229	0.0176	0.0220	0.0463
ABS	0.0156	0.0190	0.0120	0.0229	0.0176	0.0137	0.0069
1BN	0.0156	0.0171	0.0133	0.0227	0.0174	0.0162	0.0071
3BN	0.0155	0.0153	0.0144	0.0181	0.0172	0.0164	0.0073
5BN	0.0154	0.0155	0.0165	0.0173	0.0168	0.0184	0.0100
10BN	0.0155	0.0140	0.0214	0.0135	0.0161	0.0193	0.0139
20BN	0.0154	0.0117	0.0292	0.0099	0.0148	0.0195	0.0250
30BN	0.0153	0.0117	0.0342	0.0090	0.0136	0.0220	0.0463

alternatives for the seven specified performance criteria, which are summarized in a decision matrix for ARAS analysis.

In Table 4, A0 represents the optimal values (d_{0j}) as determined using Eq. (8). According to Eq. (9), normalization of the decision matrix was performed and demonstrated in Table 5. After that, the weighted normalized matrix (as shown in Table 5) is obtained using Eq. (10) and the criteria weights given in Table 6.

The optimality functions (μ_i) are determined for each alternative using Table 6 and Eq. (11) as follows:

$$\mu_{A0} = 0.0156 + 0.019 + \cdots + 0.0176 + \cdots + 0.0463 = 0.1776$$

$$\mu_{ABS} = 0.0156 + 0.019 + \cdots + 0.0176 + \cdots + 0.0069 = 0.1077$$

$$\mu_{1BN} = 0.0156 + 0.0171 + \cdots + 0.0174 + \cdots + 0.0071 = 0.1094$$

$$\mu_{30BN} = 0.0153 + 0.0117 + \cdots + 0.0136 + \cdots + 0.0463 = 0.1521$$

Table 7 displays the calculated alternative μ_i values. Finally, using Eq. (12), the utility degree (θ_i) was determined by taking the μ_{A0} as the best value as follows:

$$\theta_{A0} = \frac{0.1776}{0.1776} = 1$$

$$\theta_{ABS} = \frac{0.1077}{0.1776} = 0.6064$$

$$\theta_{1BN} = \frac{0.1094}{0.1776} = 0.6160$$

$$\theta_{30BN} = \frac{0.1521}{0.1776} = 0.8564$$

The θ_i values and associated rank for each alternative are displayed in Table 7. The utility degree (θ_i) for alternative 30BN was determined to be the highest performing (0.8564), followed by alternative 20BN ($\theta_i = 0.7066$), and finally alternative 3BN ($\theta_i = 0.5867$). Therefore, the formulation 30BN (containing ABS = 70% and boron nitride = 30% by volume) is considered the best material candidate for a given application.

Table 7 – ARAS results.

Alternatives	μ_i	θ_i	Rank
Optimum, A0	0.1776	1.0000	
ABS	0.1077	0.6064	6
1BN	0.1094	0.6160	5
3BN	0.1042	0.5867	7
5BN	0.1099	0.6188	4
10BN	0.1137	0.6402	3
20BN	0.1255	0.7066	2
30BN	0.1521	0.8564	1

3.3. *Rank validation and weight sensitivity*

3.3.1. *Rank validation using other MCDM approaches*

It is crucial to ascertain whether the recommended MCDM model satisfies the literature's requirements before making a final choice. The ranking outcomes of the suggested ARAS approach were contrasted with other decision-making approaches such as SAW, WASPAS, VIKOR, COPRAS, MOORA, and MEW, as shown in Fig. 6. In the ranks of the alternatives utilizing the various MCDM techniques demonstrate that 30BN is the most dominant (first-ranked) option. Simultaneously, 3BN is the weakest choice, ranking last among all other employed MCDM techniques except MEW, which replaces it with ABS. The results revealed that COPRAS, WASPAS, and MOORA did not affect ranking, whilst VIKOR, SAW, and MEW approaches had a minor effect on ranking. It was also established, through Eq. (14), whether or not the ranking outcomes of the recommended MCDM models were significantly different from those of the other decision-making tools. The results reveal a statistical correlation larger than 0.93, allowing us to conclude that the ranking achieved is credible and accurate.

3.3.2. *Weight sensitivity analysis*

Any MCDM method may produce erroneous or inconsistent findings under certain conditions, for example, when the weighting of criteria is modified to accommodate the evolving viewpoints of the experts. Therefore, it is essential to do a sensitivity analysis to assess the robustness of the MCDM results. The effect of exchanging the criteria weights to rank the alternatives was analyzed in a sensitivity study. There are seven criteria (C1–C7), allowing for twenty-one possible swaps. Fig. 7 displays the equivalent ranking of 21 weight exchanges after being analyzed with the ARAS approach. Alternative 30BN consistently occupies the top spot in all weight exchange sets, followed by alternatives 20BN and 10BN in all exchanges. While 3BN remained the least preferred alternative among all weight exchange sets. Overall, some sensitivity was noticed as alternatives ABS, 1BN, and 5BN switched places; however, because the ultimate aim is to pick the best option, these changes had minimal influence on the rank results. Rank sensitivity is further confirmed by the statistical correlation computed using Eq. (14). For all situations, the estimated correlation value is more than 0.89, suggesting

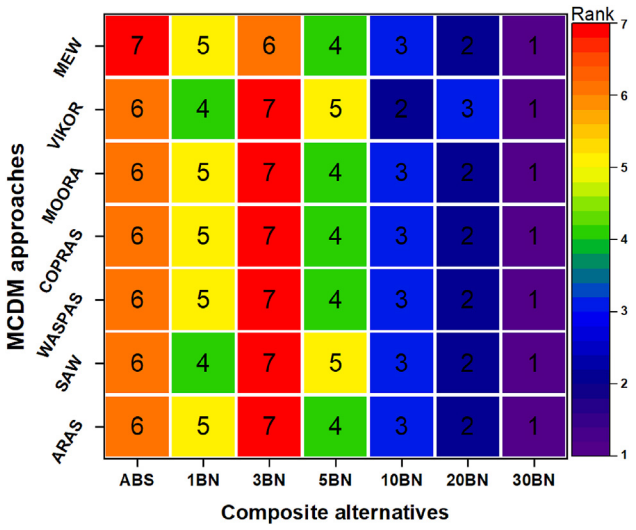

Fig. 6 – Rank validation using various MCDM approaches.

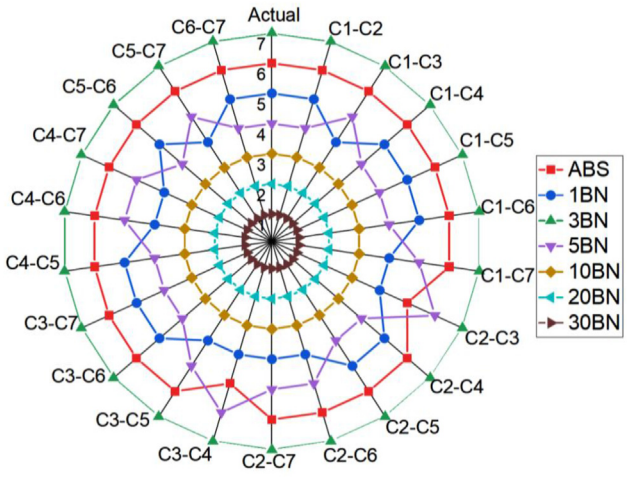

Fig. 7 – Sensitivity analysis.

that the ranking results are credible. This demonstrates the resilience of the integrated CRITIC-ARAS method for selecting the best alternatives among ABS composite materials available.

4. Conclusions

In the current study, a decision-assistance method is proposed for thermally conductive and electrically resistive polymer composite materials based on ABS matrix filled with 0, 1, 3, 5, 10, 20, and 30 vol% of BN particles. The ABS/BN composites were fabricated by melt compounding in an internal mixer followed by compression molding. Subsequently, samples were analyzed for their thermal conductivity, electrical resistivity, density, hardness, and tensile properties. According to the results there is barely any compositional dependence of hardness. Whilst, the thermal conductivity, the electrical resistivity, and Young's modulus improved with growing BN-content, at the same time the tensile strength, elongation at break, and density deteriorated. Considering these inconsistencies in the properties, it was rather difficult to prioritize the composites according to their performance and choose the best alternative.

Therefore, through the combination of the CRITIC and ARAS approaches, a hybrid decision-making technique was applied. The CRITIC technique was used to determine the weights of the analyzed attributes, and ARAS was used to obtain a preference order of the developed composites. According to the adopted techniques, the sample containing 30 vol% BN has optimal properties. A sensitivity study revealed that the ranking was not considerably influenced by changing the criteria weights. The obtained ranking was also validated through other decision-making techniques, and the results of the proposed CRITIC-ARAS approach proved reliable based on those.

Declaration of competing interest

The authors declare that they have no known competing financial interests or personal relationships that could have appeared to influence the work reported in this paper.

Acknowledgments

L. Lendvai is grateful for the support of the Hungarian Eötvös Scholarship of the Tempus Foundation. The research presented in this paper was also funded by the "Thematic Excellence Programme 2021 (TKP2021) – National Defence, National Security Subprogramme at the Széchenyi István University (TKP2021-NVA-23).

REFERENCES

[1] Jin S-W, Jin Y-J, Choi Y-J, Kim D-B, Yoon K-H, Kim H-W, et al. Eco-friendly preparation and characterization of highly thermally conductive polyimide/boron nitride composites. Compos Appl Sci Manuf 2023;166:107396.
[2] Wu X, Liu W, Shi F-g, Yang L, Zhang C. Constructing three-dimensional boron nitride network for highly thermally conductive epoxy resin composites. Polym Compos 2022;43:1711–7.
[3] Hassan M, Gondal MA, Cevik E, Qahtan TF, Bozkurt A, Dastageer MA. High performance pliable supercapacitor fabricated using activated carbon nanospheres intercalated into boron nitride nanoplates by pulsed laser ablation technique. Arab J Chem 2020;13:6696–707.
[4] Wu W, Zheng M, Lu K, Liu F, Song Y-H, Liu M, et al. Thermally conductive composites based on hexagonal boron nitride nanosheets for thermal management: fundamentals to applications. Compos Appl Sci Manuf 2023;169:107533.
[5] Wang Z, Wang X, Zhang Z, Liang L, Zhao Z, Shi J. Preparation of a 3D BN network structure by a salt-template-assisted method filled with epoxy resin to obtain high thermal conductivity nanocomposites. Polym Compos 2023;44:3610–21.
[6] Cui Y, Xu F, Bao D, Gao Y, Peng J, Lin D, et al. Construction of 3D interconnected boron nitride/carbon nanofiber hybrid

network within polymer composite for thermal conductivity improvement. J Mater Sci Technol 2023;147:165–75.
[7] Bragaglia M, Lamastra FR, Russo P, Vitiello L, Rinaldi M, Fabbrocino F, et al. A comparison of thermally conductive polyamide 6-boron nitride composites produced via additive layer manufacturing and compression molding. Polym Compos 2021;42:2751–65.
[8] Alam F, Choosri M, Gupta TK, Varadarajan KM, Choi D, Kumar S. Electrical, mechanical and thermal properties of graphene nanoplatelets reinforced UHMWPE nanocomposites. Mater Sci Eng, B 2019;241:82–91.
[9] Pan X, Shen L, Schenning APHJ, Bastiaansen CWM. Transparent, high-thermal-conductivity ultradrawn polyethylene/graphene nanocomposite films. Adv Mater 2019;31:1904348.
[10] Ouyang Y, Ding F, Bai L, Li X, Hou G, Fan J, et al. Design of network Al2O3 spheres for significantly enhanced thermal conductivity of polymer composites. Compos Appl Sci Manuf 2020;128:105673.
[11] Liu D, Ma C, Chi H, Li S, Zhang P, Dai P. Enhancing thermal conductivity of polyimide composite film by electrostatic self-assembly and two-step synergism of Al2O3 microspheres and BN nanosheets. RSC Adv 2020;10:42584–95.
[12] Li K, Liu Y, Wang S, Jin X, Li W, Gan W, et al. Construction of 3D framework of BN and silica with advanced thermal conductivity of epoxy composites. J Polym Res 2023;30:219.
[13] Yuan Y, Hu H, Wu W, Zhao Z, Du X, Wang Z. Hybrid of multi-dimensional fillers for thermally enhanced polyamide 12 composites fabricated by selective laser sintering. Polym Compos 2021;42:4105–14.
[14] Lendvai L, Rigotti D. Thermal and thermomechanical properties of boron nitride-filled acrylonitrile butadiene styrene (ABS) composites. Acta Technica Jaurinensis 2023;16:123–8.
[15] Khan A, Puttegowda M, Jagadeesh P, Marwani HM, Asiri AM, Manikandan A, et al. Review on nitride compounds and its polymer composites: a multifunctional material. J Mater Res Technol 2022;18:2175–93.
[16] Lule Z, Kim J. Thermally conductive and highly rigid polylactic acid (PLA) hybrid composite filled with surface treated alumina/nano-sized aluminum nitride. Compos Appl Sci Manuf 2019;124:105506.
[17] Wu G, Wang Y, Wang K, Feng A. The effect of modified AlN on the thermal conductivity, mechanical and thermal properties of AlN/polystyrene composites. RSC Adv 2016;6:102542–8.
[18] Qian M, Song P, Qin Z, Yan S, Zhang L. Mechanically robust and abrasion-resistant polymer nanocomposites for potential applications as advanced clearance joints. Compos Appl Sci Manuf 2019;126:105607.
[19] Kovacs J, Suplicz A. Thermally conductive polymer compounds for injection moulding: the synergetic effect of hexagonal boron-nitride and talc. J Reinforc Plast Compos 2013;32:1234–40.
[20] Cheewawuttipong W, Fuoka D, Tanoue S, Uematsu H, Iemoto Y. Thermal and mechanical properties of polypropylene/boron nitride composites. Energy Proc 2013;34:808–17.
[21] Gurgenc T, Biryan F. Production, thermal and dielectrical properties of Ag-doped nano-strontium apatite and nano h-BN filled poly(4-(3-(2,3,4-trimethoxyphenyl) acryloyl) phenyl acrylate) composites. J Polym Res 2020;27:194.
[22] Wei S-N, Liu X, Yan J, Zhong M, Joseph P, Zhang J, et al. A study of the mechanical performance of nanocomposites of polyethylene containing exfoliated boron nitride nanoplatelets. Polym Compos 2022;43:6276–86.
[23] Li G, Xing R, Geng P, Liu Z, He L, Wang N, et al. Surface modification of boron nitride via poly (dopamine) coating and preparation of acrylonitrile-butadiene-styrene copolymer/boron nitride composites with enhanced thermal conductivity. Polym Adv Technol 2018;29:337–46.
[24] Waheed S, Cabot JM, Smejkal P, Farajikhah S, Sayyar S, Innis PC, et al. Three-dimensional printing of abrasive, hard, and thermally conductive synthetic microdiamond–polymer composite using low-cost fused deposition modeling printer. ACS Appl Mater Interfaces 2019;11:4353–63.
[25] Singh T, Fekete I, Jakab SK, Lendvai L. Selection of straw waste reinforced sustainable polymer composite using a multi-criteria decision-making approach. Biomass Conversion and Biorefinery; 2023.
[26] Singh T, Pattnaik P, Shekhawat D, Ranakoti L, Lendvai L. Waste marble dust-filled sustainable polymer composite selection using a multi-criteria decision-making technique. Arab J Chem 2023;16:104695.
[27] Singh S, Doddamani M, Powar S. Multi-objective optimization of machining parameter in laser drilling of glass microballoon/epoxy syntactic foams. J Mater Res Technol 2023;23:3869–79.
[28] Oroujzadeh M, Nikouei MA, Mehdipour-Ataei S, Amiri M. Materials selection for choosing the best composite blend polymeric membrane for hydrogen/oxygen proton exchange membrane fuel cell. J Power Sources 2022;538:231566.
[29] Soni A, Chakraborty S, Kumar Das P, Kumar Saha A. Materials selection of reinforced sustainable composites by recycling waste plastics and agro-waste: an integrated multi-criteria decision making approach. Construct Build Mater 2022;348:128608.
[30] Singh T. Optimum design based on fabricated natural fiber reinforced automotive brake friction composites using hybrid CRITIC-MEW approach. J Mater Res Technol 2021;14:81–92.
[31] Akbar A, Liew KM. Multicriteria performance evaluation of fiber-reinforced cement composites: an environmental perspective. Compos B Eng 2021;218:108937.
[32] Zavadskas EK, Turskis Z, Vilutiene T. Multiple criteria analysis of foundation instalment alternatives by applying Additive Ratio Assessment (ARAS) method. Arch Civ Mech Eng 2010;10:123–41.
[33] Khargotra R, Kumar R, Sharma A, Singh T. Design and performance optimization of solar water heating system with perforated obstacle using hybrid multi-criteria decision-making approach. J Energy Storage 2023;63:107099.
[34] Büyüközkan G, Güler M. Smart watch evaluation with integrated hesitant fuzzy linguistic SAW-ARAS technique. Measurement 2020;153:107353.
[35] Balki MK, Erdoğan S, Aydın S, Sayin C. The optimization of engine operating parameters via SWARA and ARAS hybrid method in a small SI engine using alternative fuels. J Clean Prod 2020;258:120685.
[36] Fu Y-K. An integrated approach to catering supplier selection using AHP-ARAS-MCGP methodology. J Air Transport Manag 2019;75:164–9.
[37] Mishra AR, Rani P, Cavallaro F, Mardani A. A similarity measure-based Pythagorean fuzzy additive ratio assessment approach and its application to multi-criteria sustainable biomass crop selection. Appl Soft Comput 2022;125:109201.
[38] Ghenai C, Albawab M, Bettayeb M. Sustainability indicators for renewable energy systems using multi-criteria decision-making model and extended SWARA/ARAS hybrid method. Renew Energy 2020;146:580–97.
[39] Diakoulaki D, Mavrotas G, Papayannakis L. Determining objective weights in multiple criteria problems: the critic method. Comput Oper Res 1995;22:763–70.

[40] Menekşe A, Camgöz Akdağ H. Medical waste disposal planning for healthcare units using spherical fuzzy CRITIC-WASPAS. Appl Soft Comput 2023;144:110480.
[41] Aytekin A, Okoth BO, Korucuk S, Mishra AR, Memiş S, Karamaşa Ç, et al. Critical success factors of lean six sigma to select the most ideal critical business process using q-ROF CRITIC-ARAS technique: case study of food business. Expert Syst Appl 2023;224:120057.
[42] Jovčić S, Průša P. A hybrid MCDM approach in third-party logistics (3PL) provider selection. Mathematics 2021;9:2729.
[43] Sultana MN, Ranjan Dhar N. RSM design-based hybrid approach to multi-response optimization in milling Ti-6Al-4 V alloy: a comparative study. Mater Today Proc 2023;9:e18582.
[44] Ayyıldız TE, Ekinci EBM. Selection of Six Sigma projects based on integrated multi-criteria decision-making methods: the case of the software development industry. J Supercomput 2023;79:14981–5003.
[45] Shiva Kumar K, Chennakesava Reddy A. Investigation on mechanical properties and wear performance of Nylon-6/ Boron Nitride polymer composites by using Taguchi Technique. Results in Materials 2020;5:100070.
[46] Zheng J, He S, Wang J, Fang W, Xue Y, Xie L, et al. Performance of silicone rubber composites filled with aluminum nitride and alumina tri-hydrate. Materials 2020;13:2489.
[47] Ghaffari Mosanenzadeh S, Liu MW, Osia A, Naguib HE. Thermal composites of biobased polyamide with boron nitride micro networks. J Polym Environ 2015;23:566–79.
[48] Chen J, Zhu J, Pan Y, Wu H, Guo S, Qiu J. Fabrication of wear-resistant PA6 composites with superior thermal conductivity and mechanical properties via constructing highly oriented hybrid network of SiC-packed BN platelets. J Mater Sci Technol 2023;146:200–10.
[49] Zhou W, Zuo J, Zhang X, Zhou A. Thermal, electrical, and mechanical properties of hexagonal boron nitride–reinforced epoxy composites. J Compos Mater 2014;48:2517–26.
[50] Fu S-Y, Feng X-Q, Lauke B, Mai Y-W. Effects of particle size, particle/matrix interface adhesion and particle loading on mechanical properties of particulate–polymer composites. Compos B Eng 2008;39:933–61.
[51] Watanabe K, Taniguchi T, Kanda H. Direct-bandgap properties and evidence for ultraviolet lasing of hexagonal boron nitride single crystal. Nat Mater 2004;3:404–9.
[52] Song L, Ci L, Lu H, Sorokin PB, Jin C, Ni J, et al. Large scale growth and characterization of atomic hexagonal boron nitride layers. Nano Lett 2010;10:3209–15.
[53] Li LH, Santos EJG, Xing T, Cappelluti E, Roldán R, Chen Y, et al. Dielectric screening in atomically thin boron nitride nanosheets. Nano Lett 2015;15:218–23.
[54] Yuan H, Wang Y, Li T, Wang Y, Ma P, Zhang H, et al. Fabrication of thermally conductive and electrically insulating polymer composites with isotropic thermal conductivity by constructing a three-dimensional interconnected network. Nanoscale 2019;11:11360–8.
[55] Li H, Xie Z, Liu L, Peng Z, Ding Q, Ren L, et al. High-performance insulation materials from poly(ether imide)/ boron nitride nanosheets with enhanced DC breakdown strength and thermal stability. IEEE Trans Dielectr Electr Insul 2019;26:722–9.
[56] Xie Y, Wang J, Yu Y, Jiang W, Zhang Z. Enhancing breakdown strength and energy storage performance of PVDF-based nanocomposites by adding exfoliated boron nitride. Appl Surf Sci 2018;440:1150–8.
[57] Bayır S, Semerci E, Erdogan Bedri T. Preparation of novel thermal conductive nanocomposites by covalent bonding between hexagonal boron nitride nanosheet and well-defined polymer matrix. Compos Appl Sci Manuf 2021;146:106406.
[58] Zhou W, Qi S, An Q, Zhao H, Liu N. Thermal conductivity of boron nitride reinforced polyethylene composites. Mater Res Bull 2007;42:1863–73.
[59] Ishida H, Rimdusit S. Very high thermal conductivity obtained by boron nitride-filled polybenzoxazine. Thermochim Acta 1998;320:177–86.
[60] Sato K, Horibe H, Shirai T, Hotta Y, Nakano H, Nagai H, et al. Thermally conductive composite films of hexagonal boron nitride and polyimide with affinity-enhanced interfaces. J Mater Chem 2010;20:2749–52.